Article

*Discovery Medicine* 2025; 37(203): 3095–3106
https://doi.org/10.24976/Discov.Med.202537203.259

# Protective Effects of Propofol on Acute Kidney Injury Through Suppressing Ferroptosis and Inflammatory Responses in Renal Tubular Epithelial Cells

Jie Li[1], Huanhuan Zhang[2,*]

[1]Department of Anesthesiology, Yantaishan Hospital, 264001 Yantai, Shandong, China
[2]Department of Nephrology, Linyi Hospital of Traditional Chinese Medicine, 276000 Linyi, Shandong, China
*Correspondence: z15910131104@163.com (Huanhuan Zhang)
Submitted: 28 October 2025 Revised: 27 November 2025 Accepted: 8 December 2025 Published: 20 December 2025

**Background: Acute kidney injury (AKI) poses a serious threat to patients' health, creating an urgent need for effective prevention and treatment strategies. Propofol, an anesthetic used in clinical practice, has demonstrated protective effects across several organs. This study aims to explore the effect of propofol on AKI and its underlying mechanism.**

**Methods: An AKI model was established by using lipopolysaccharide (LPS) injection. At 24 hours post-operation, renal function was evaluated through biochemical analyzers and hematoxylin-eosin staining. The level of oxidative stress was detected using a biochemical kit. Iron death-related proteins in kidney tissues were evaluated by Western blot (WB) analysis, and iron deposition was observed by Perls staining. The levels of inflammatory factors were detected by Enzyme-linked immunosorbent assay (ELISA) and immunohistochemistry. *In vitro* experiments were performed using human proximal tubular epithelial cells (HK-2). Cell viability was detected by Cell Counting Kit-8 assay, intracellular reactive oxygen species (ROS) was detected by flow cytometry, and the expression of ferroptosis-related proteins was determined by WB.**

**Results: In the *in vivo* experiments, propofol treatment significantly improved renal function ($p < 0.05$). The indicators related to oxidative stress and ferroptosis were downregulated ($p < 0.05$). The levels of inflammatory factors were reduced, and the activation of the inflammatory body was suppressed ($p < 0.05$). The *in vitro* experiments showed that propofol could significantly increase the cell viability of HK-2 ($p < 0.05$), reduce ROS production ($p < 0.05$), downregulate ferroptosis-related proteins levels ($p < 0.05$), and inflammatory responses ($p < 0.05$). Upon induction of ferroptosis with Erastin, the protective effect of propofol was attenuated ($p < 0.05$).**

**Conclusions: Propofol has a significant protective effect on AKI, mainly through inhibiting ferroptosis and inflammatory responses in renal tubular epithelial cells. This research provides a strong theoretical basis and experimental foundation for the clinical application of propofol in the prevention and treatment of AKI.**

**Keywords:** propofol; acute kidney injury; ferroptosis; inflammatory; oxidative stress

## Introduction

Acute Kidney Injury (AKI) has emerged as a critical challenge in the field of clinical critical care, with incidence rates rising annually, posing a serious threat to patients' lives and health [1]. Epidemiological data indicate that the prevalence of AKI among hospitalized patients ranges from approximately 10%–15% globally, while in the Intensive Care Unit (ICU), this proportion is as high as over 50% [2]. Although modern medicine has seen continuous advances in diagnostic and therapeutic techniques, the short-term mortality of patients with AKI remains a significant challenge. Moreover, the risk of subsequent development into chronic kidney disease or cardiovascular complications for survivors is significantly increased [3]. Therefore, delving into the pathogenesis of AKI and seeking effective prevention and treatment strategies has become a key issues that urgently need to be addressed.

At present, the pathogenesis of AKI is extremely complex. It typically includes cellular dysfunction, hypoxia, mitochondrial damage, renal tubular injury, and dysregulation of the inflammatory response [4,5]. Among them, the renal tubular epithelial cells, being an important foundation of the kidneys, play a central role in the occurrence and development of AKI [6]. When the kidneys are subjected to damage factors such as ischemia-reperfusion injury (IRI), nephrotoxic substances, and drugs, the epithelial cells of the renal tubules bear the brunt. Their normal physiological functions are disrupted, resulting in damage to the structural integrity of the renal tubules and subsequently leading to a sharp decline in renal function [7,8]. Recently, there has been a growing interest in investigating new types of cell death, such as necroptosis, pyroptosis, and ferroptosis etc [8–12]. Among them, ferroptosis has gradually become a research hotspot due to its unique molecular mechanism

and crucial role in kidney diseases [13]. For instance, research has shown that inhibiting the long-chain family 4 of acyl-CoA synthetase (ACSL4) can alleviate ferroptosis and significantly reduce the severity of AKI, as well as improve renal function [14]. In the AKI model induced by sepsis, the use of Ferrostatin-1 can reduce the death of proximal tubular cells in mice, and lower the levels of glutathione peroxidase 4 (GPX4), malondialdehyde (MDA), 4-hydroxynonenal (4-HNE), and reactive oxygen species (ROS) [15]. In addition, the inflammatory response also exerts a significant influence on AKI [16]. When the kidneys are damaged, the epithelial cells of the renal tubules and immune cells are activated, releasing inflammatory factors including tumor necrosis factor-$\alpha$ (TNF-$\alpha$), interleukin-1$\beta$ (IL-1$\beta$), and interleukin-6 (IL-6), which trigger an inflammatory cascade reaction, further aggravating the damage to the kidney tissues [17].

Propofol is a widely used intravenous anesthetic, commonly employed for the sedation of ICU patients and anesthesia for outpatient surgeries. Besides its anesthetic effects, an increasing number of studies in recent years have demonstrated that propofol has extensive organ-protective properties, including for the heart, liver, brain, lungs, and other vital organs [18–21]. Research has found that propofol can inhibit oxidative stress and inflammatory responses to alleviate cerebral IRI [22]. In terms of liver protection, propofol can alleviate liver damage by regulating cytochrome activity and inhibiting hepatocyte apoptosis [23]. There have been some preliminary research reports regarding the protective effect of propofol on the kidneys. For instance, in the rat model of renal IRI, propofol alleviates and improves renal function. The mechanism may be pertinent to the inhibition of oxidative stress, inflammatory response, and cell apoptosis [24]. In sepsis-induced AKI mice, propofol inhibits inflammatory factors by upregulating miR-290-5p, thereby improving AKI and survival outcomes in these septic mice [25]. Propofol also inhibits the pro-apoptotic proteins and inflammatory factors, and plays an anti-apoptotic and anti-inflammatory protective role in renal tissues [26]. However, the effect of propofol on AKI induced by lipopolysaccharide (LPS) and its specific mechanism, especially the influence on ferroptosis and inflammatory response of renal tubular epithelial cells, is still not fully clear.

Given the above, this study aims to focus on the influence of propofol on ferroptosis and inflammatory responses in renal tubular epithelial cells, providing a theoretical and experimental basis for AKI and supporting the development of novel therapeutic approaches for AKI.

## Materials and Methods

### *Experimental Animal Models*

In this experiment, 6–8-week-old male C57BL/6 mice (20–25 g) were purchased from Cyagen (Suzhou, China). All mice had free access to food and water, and maintained a 12-hour light/12-hour dark daily cycle. The experimental protocol was approved by the Ethics Committee of Beijing Keweite Laboratory Animal Welfare (Approval No. KWT-2024-0112-01) and followed the relevant ethical guidelines for the care and use of laboratory animals. The mice were randomly divided into the following 4 groups, with 6 mice in each group: Control group (Con): Only underwent surgical exposure of the kidneys and received sterile normal saline; Propofol group (Pro): Received intraperitoneal injections of propofol (50 mg/kg, mixed with intralipid), twice within 24 hours, to observe the effect of propofol alone on the mice [19]; AKI model group (AKI): Received intravenous injection of LPS (5 mg/kg, dissolved in physiological saline) through the tail vein [27]; AKI + propofol intervention group (AKI + Pro): Intraperitoneal injections of propofol (50 mg/kg) were administered twice within 24 hours. One hour after the last injection, intravenous injection of LPS (5 mg/kg) was given through the tail vein to construct the AKI model. At the end of the experiment (24 hours after modeling), the mice were euthanized by intraperitoneal injection of an excessive dose of pentobarbital sodium at a dose of 150 mg/kg. After euthanasia, the serum (rapid cardiac puncture), urine, and kidney tissues of the mice were collected for subsequent experiments [28].

### *Renal Function Assessment*

The mouse models were established after 24 hours, the mice were individually housed in metabolic cages for another 24 hours, and all the urine samples were collected for relevant tests. The urine protein content was detected using the Enzyme-linked immunosorbent assay (ELISA) urine protein test kit (CB10528-Mu, CPIBO BIO, Shanghai, China). The specific steps are as follows: The urine was collected in a sterile tube and centrifuged for about 20 minutes (at 2000–3000 revolutions per minute) following the instructions of the kit. The values on the microplate reader were read, and the urine protein content was calculated based on the standard curve. After the mice were euthanized, rapid cardiac puncture was performed to collect blood. The blood was then centrifuged (at 3000 rpm for 10 minutes) to separate the serum. The Scr and BUN levels in serum were detected using an automatic biochemical analyzer (Chemray 240, Rayto, Shenzhen, China) to evaluate the renal function of the mice.

### *Histopathological Analysis*

The fixed renal tissues were successively subjected to dehydration, paraffin embedding, and sectioning (thickness 4 μm), and then stained with Hematoxylin-Eosin (HE). After staining, the slides were sealed and observed under a microscope (Nikon Eclipse E100, Nikon, Tokyo, Japan). A semi-quantitative scoring system was used to score the indicators, such as tubular epithelial cell swelling, brush

border shedding, tubular cast formation, and cell necrosis. The scoring criteria are as follows: 0 points, no damage; 1 point, <25% tubular damage; 2 points, 25%–50% tubular damage; 3 points, 50%–75% tubular damage; 4 points, >75% tubular damage [29]. The histopathological scores were independently assigned by two pathologists who were unaware of the experimental groups, using a double-blind method.

### *Oxidative Stress Level Detection*

The levels of ROS (BC-K138-F), MDA (E-BC-K027-S), and 4-HNE (E-EL-0128c) in renal tissues were detected by a commercial kit (Elabscience, Wuhan, China) to assess the degree of oxidative stress. Renal tissue was harvested, and pre-cooled homogenization buffer was added. The tissue was homogenized under ice bath conditions, and then centrifuged for 10 minutes (4 °C, 12000 rpm) before extracting the supernatant for detection. The specific operation steps were carried out strictly in accordance with the kit instructions.

### *Detection of Ferroptosis-related Proteins*

The expression levels of GPX4 and ACSL4 proteins in kidney tissue and human proximal tubular epithelial cells (HK-2) were detected using Western blot (WB) analysis in accordance with a previously published technique [30]. RIPA lysis buffer (P0013J, Beyoyime, Shanghai, China) containing protease inhibitors and phosphatase inhibitors was added. Equal amounts of protein underwent electrophoresis and transfer to the membrane. Then primary antibodies (GPX4 antibody, A11243, 1:1000, ABclonal; ACSL4 antibody, ET7111-43, 1:1000, Huabio; GAPDH antibody, 60004-1-Ig, 1:5000; Proteintech) were added and incubated. The next day, secondary antibodies (goat anti-rabbit IgG, ZB-2301, 1:2000; goat anti-mouse IgG, ZB-2305, 1:2000; ZSBIO) were added and incubated for 1 hour. The image was captured using a Gel Imaging System (Tanon-4600, Tanon, Shanghai, China), and the protein band gray value was analyzed using ImageJ software (National Institutes of Health, MD, USA).

### *Iron Deposition Detection*

The Perls Prussian blue staining kit (G1029, Servicebio, Wuhan, China) was used to detect the iron deposition in renal tubular epithelial cells. Paraffin sections were deparaffinized and rehydrated to water, incubated with Perls Prussian blue staining solution for 60 minutes, washed with water, dehydrated, cleared, and mounted. The samples were observed under a microscope. The iron deposition sites appeared blue, and the number of positive cells was calculated.

### *The Detection of Inflammatory Factors*

The levels of TNF-$\alpha$ (E-MSEL-M0002), IL-1$\beta$ (E-MSEL-M0003), and IL-6 (E-MSEL-M0001) in serum and kidney tissue homogenate were detected using the ELISA method. Appropriate amounts of serum or supernatant of kidney tissue homogenate were taken, and the detection was carried out according to the manufacturer's instructions of the ELISA kit (Elabscience, Wuhan, China). The concentrations of inflammatory factors were calculated based on the standard curve.

### *Immunohistochemistry*

The paraffin sections were deparaffinized and rehydrated to water, blocked with 3% hydrogen peroxide solution for 10 minutes, and 5% goat serum for 30 minutes. The NOD-like receptor thermal protein domain-associated protein 3 (NLRP3) antibody (GB114320, Servicebio, Wuhan, China) was added and incubated at 4 °C overnight. The next day, the sections were washed 3 times with PBS, each for 5 minutes, and then a HRP-labeled secondary antibody (goat anti-rabbit IgG, GB23303, Servicebio, Wuhan, China) was added and incubated at room temperature for 1 hour. DAB staining was performed, followed by hematoxylin counterstaining, dehydration, transparency, and mounting. The samples were observed under a microscope. The immunohistochemical staining images were quantitatively analyzed using ImageJ software, and the detection index was integral optical density (IOD/area).

### *Cell Culture*

Human proximal renal tubular epithelial cells (HK-2, CBP60447) and the complete culture medium (CBP60447M) were all purchased from COBIOER (Nanjing, China). They were cultured in an incubator as per the manufacturer's instructions for cultivation (37 °C, 5% $CO_2$). The cells have been subjected to STR analysis and mycoplasma testing and have been confirmed to be free from contamination. The number of cell passages was within 15 generations. When the cell density reached $5\times10^5$ cells/mL, the cells were divided into the following 5 groups: Control group (Con): Normal cultured HK-2 cells without any treatment; Propofol group (Pro): 10 µM propofol was added to the culture medium and cultured for 24 hours [31]; LPS group (LPS): 1 µg/mL LPS was added to the medium and cultured for 24 hours [32]; Propofol + LPS group (Pro+LPS): 1 hour before LPS induction, 10 µM propofol was added to the cell culture medium for pretreatment, and then 1 µg/mL LPS was added for 24 hours of cultivation; Propofol+LPS+Erastin group (Pro+LPS+Erastin): Before LPS induction, the cells were pretreated with 10 µM propofol for 1 hour, and then 10 µM Erastin (a ferroptosis inducer, Selleck Chemicals, USA) and 1 µg/mL LPS were added together for 24 hours of cultivation [33].

### *Cell Viability Detection*

Cell viability was detected using the Cell Counting Kit-8 (CCK-8) method. During cell inoculation, the con-

centration was adjusted to $2 \times 10^3$ cells/mL and then added to the 96-well plate. After completing the 24-hour culture stage, 10 microliters of the CCK-8 detection solution (96992, Sigma, St. Louis, MO, USA) was injected into each well; after an interval of 2 hours, an absorption measurement was conducted using the DR-200Bs microplate reader (DR-200Bs, Diatek, Wuxi, China), at a detection wavelength of 450 nanometers.

### *Flow Cytometry*

To assess intracellular ROS levels, the DCFH-DA probe technique (S0033S, Beyotime, Shanghai, China) was utilized. Following the cultivation of cells, they were rinsed three times with PBS. Subsequently, the DCFH-DA probe was introduced, and the cells were incubated at 37 °C for 20 minutes. Afterward, the cells were washed once more to remove any excess probe. Trypsin was then used to detach the cells, which were collected as a suspension. Fluorescence intensity was measured using a flow cytometer (CytoFLEX, Beckman Coulter, Miami, FL, USA).

### *Immunofluorescence Assay*

The expression of NLRP3 in the cells was detected using the immunofluorescence method. The cells were cultured in 24-well plates with coverslips. After the treatment, the cells were fixed and permeabilized, blocked with 5% BSA for 1 hour, and then incubated with NLRP3 antibody (ET1610-93, HUABIO) at 4 °C overnight. The cells were washed with PBS and then incubated with Cy3-labeled secondary antibody (GB21303, Servicebio) at room temperature for 1 hour. The cells were washed three times with PBS and then stained with DAPI for 10 minutes. After mounting, the cells were observed under a fluorescence microscope (APX100 Olympus, Tokyo, Japan), and positive expression of NLRP3 was indicated by green fluorescence. Quantitative analysis of immunofluorescence staining images was conducted using the ImageJ software. The specific detection indicators were the average fluorescence intensity of the regions of the target protein showing positive expression. During the analysis process, at least 5 random fields of view were selected from each group.

### *Statistical Methods*

GraphPad Prism (9.0, Graphpad Software, San Diego, CA, USA) was employed for data analysis. Quantitative data are presented as mean $\pm$ standard deviation. Comparisons between two groups were performed using a *t*-test, while one-way analysis of variance (One-Way ANOVA) followed by Tukey's post-hoc test was applied for evaluating differences across multiple groups. A *p*-value below 0.05 was considered statistically significant.

## Results

### *Propofol Significantly Improves Renal Function in the AKI Model Mice*

Compared with the AKI model mice, the AKI+Pro treatment showed a marked downward trend in urinary protein content, and both Scr and BUN levels were significantly reduced, suggesting that propofol can effectively alleviate glomerular filtration dysfunction and azotemia in AKI model mice ($p < 0.05$) [Fig. 1a–c]. Renal HE staining revealed normal renal tissue morphology and intact tubular cell structures with lower renal tissue scores in the control group. In contrast, the AKI group exhibited obvious pathological changes such as tubular epithelial cell swelling, inflammatory cell infiltration, and cell necrosis, with a significantly increased tubular injury score. The AKI+Pro group showed markedly alleviated tubular structural damage, with a significantly lower tubular injury score than the AKI model group, indicating that propofol improves the renal pathological status of AKI model mice by reducing structural damage to tubular epithelial cells ($p < 0.05$) [Fig. 1d,e]. There were no significant differences in renal function indices in the propofol single-treatment, indicating that propofol has no significant effect on renal function in normal mice, and its renal function-improving effect is only evident under AKI pathological conditions.

### *Propofol Inhibits Renal Oxidative Stress and Regulates Renal Ferroptosis in AKI Model Mice*

The AKI model group exhibited significantly elevated levels of ROS, MDA, and 4-HNE in renal tissues, indicative of a markedly enhanced oxidative stress state. Conversely, the AKI+Pro group showed substantial reductions in renal ROS, MDA, and 4-HNE levels compared to the AKI model group, demonstrating that propofol effectively scavenges excessive free radicals and inhibits lipid peroxidation to alleviate renal oxidative stress injury ($p < 0.05$) [Fig. 2a–c]. WB analysis revealed a considerable downregulation of GPX4 protein expression and an upregulation of ACSL4 in AKI model renal tissues. In the AKI+Pro group, GPX4 expression was notably upregulated, while ACSL4 expression was downregulated, suggesting that propofol inhibits ferroptosis in tubular epithelial cells by modulating key ferroptosis-related proteins ($p < 0.05$) [Fig. 2d,e]. Perls staining further confirmed increased iron deposition in tubular epithelial cells of the AKI group, which was notably reduced in the AKI+Pro group, reinforcing propofol's inhibitory effect on renal ferroptosis ($p < 0.05$) [Fig. 2f,g].

### *Propofol Diminishes Renal Inflammatory Response and Inhibits NLRP3 Inflammasome Activation in AKI Model Mice*

ELISA results showed significantly elevated levels of proinflammatory cytokines (TNF-$\alpha$, IL-1$\beta$, IL-6) in serum and renal tissue homogenates of the AKI model group,

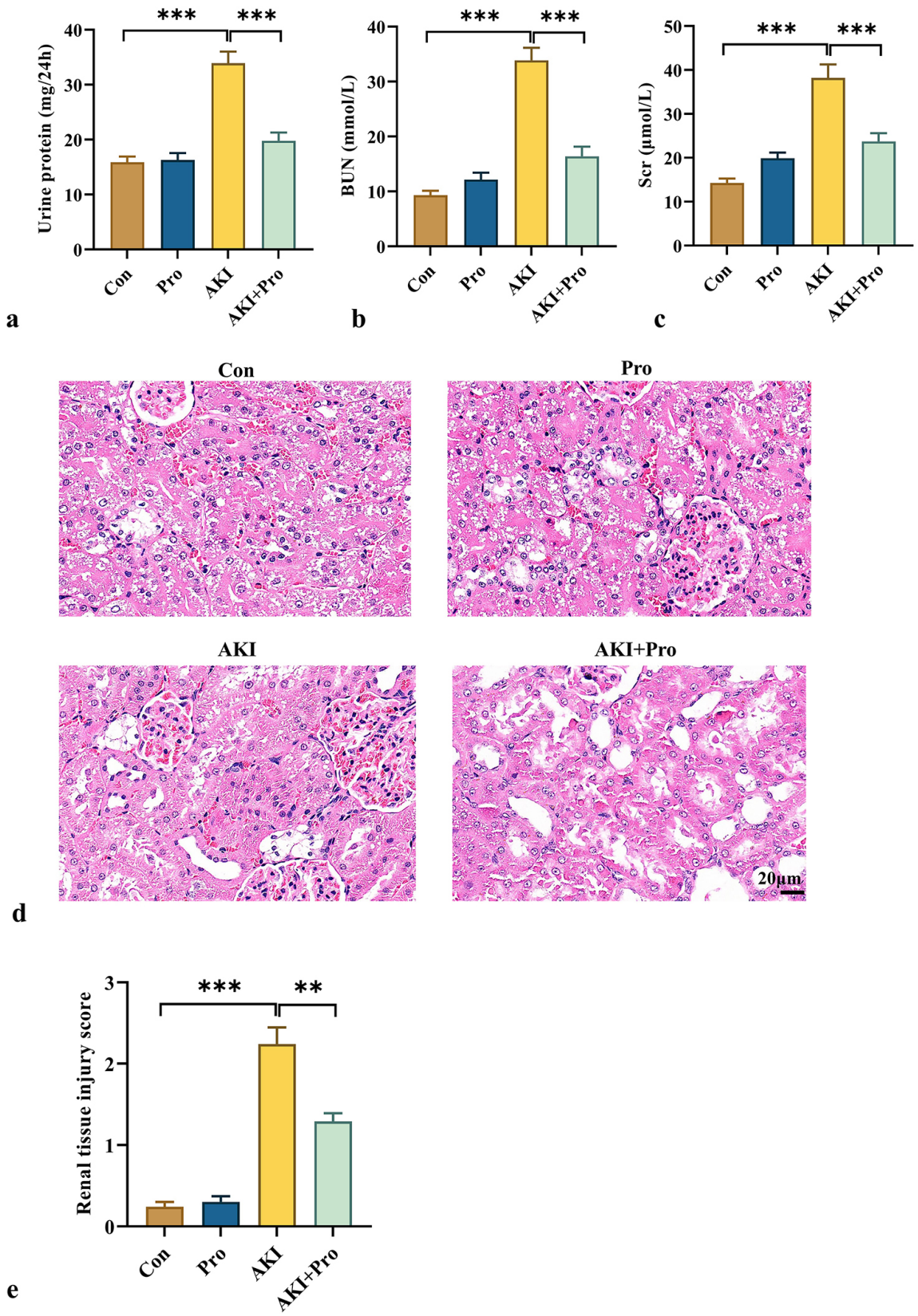


**Fig. 1. Propofol significantly improves renal function in AKI model mice.** (a–c) Urine protein, BUN, and Scr levels were detected using ELISA. (d) Representative images of HE staining of renal tissues from each group (scale bar: 20 μm, magnification ×400). (e) The renal tissue injury scores of each group of mice. n = 6; $^{**}p < 0.01$, $^{***}p < 0.001$.

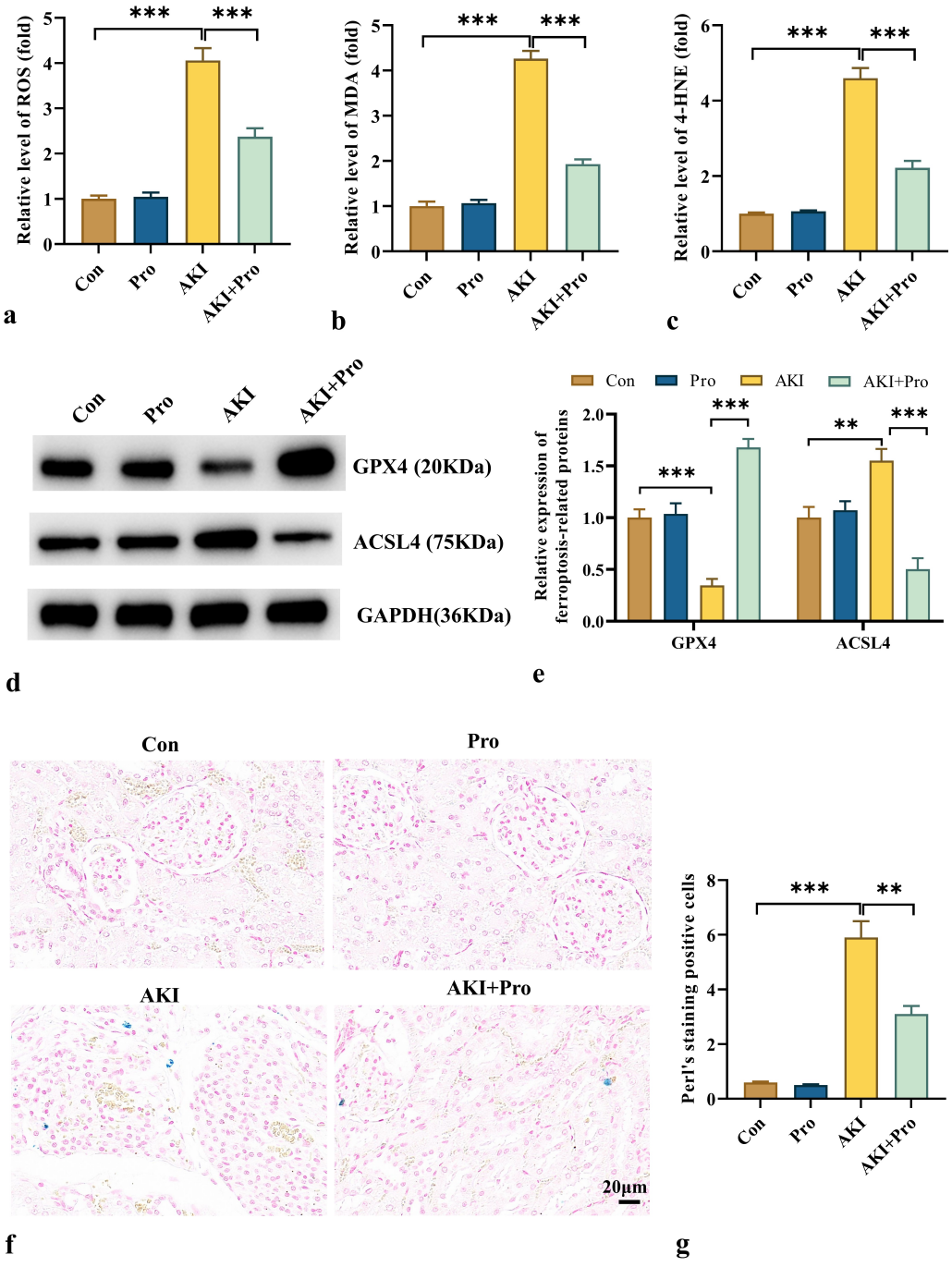


**Fig. 2. Propofol inhibits renal oxidative stress and regulates renal ferroptosis in AKI model mice.** (a–c) The renal ROS, MDA, and 4-HNE levels were detected. (d,e) WB analysis was used to detect the protein levels of GPX4 and ACSL4. (f,g) The iron deposition levels in each group were observed using Perls staining (scale bar: 20 μm, magnification ×400). n = 6; $^{**}p < 0.01$, $^{***}p < 0.001$.

whereas the AKI+Pro group exhibited substantial reductions in these inflammatory markers, indicating propofol's efficacy in inhibiting cytokine release ($p < 0.05$) [Fig. 3a–f]. Immunohistochemical analysis revealed a marked increase in NLRP3 inflammasome-positive cells in AKI model renal tissues, while the AKI+Pro group showed a considerable decrease in both the number of positive cells and staining intensity, suggesting that propofol alleviates renal inflammatory injury by suppressing NLRP3 inflammasome activation ($p < 0.05$) [Fig. 3g,h].

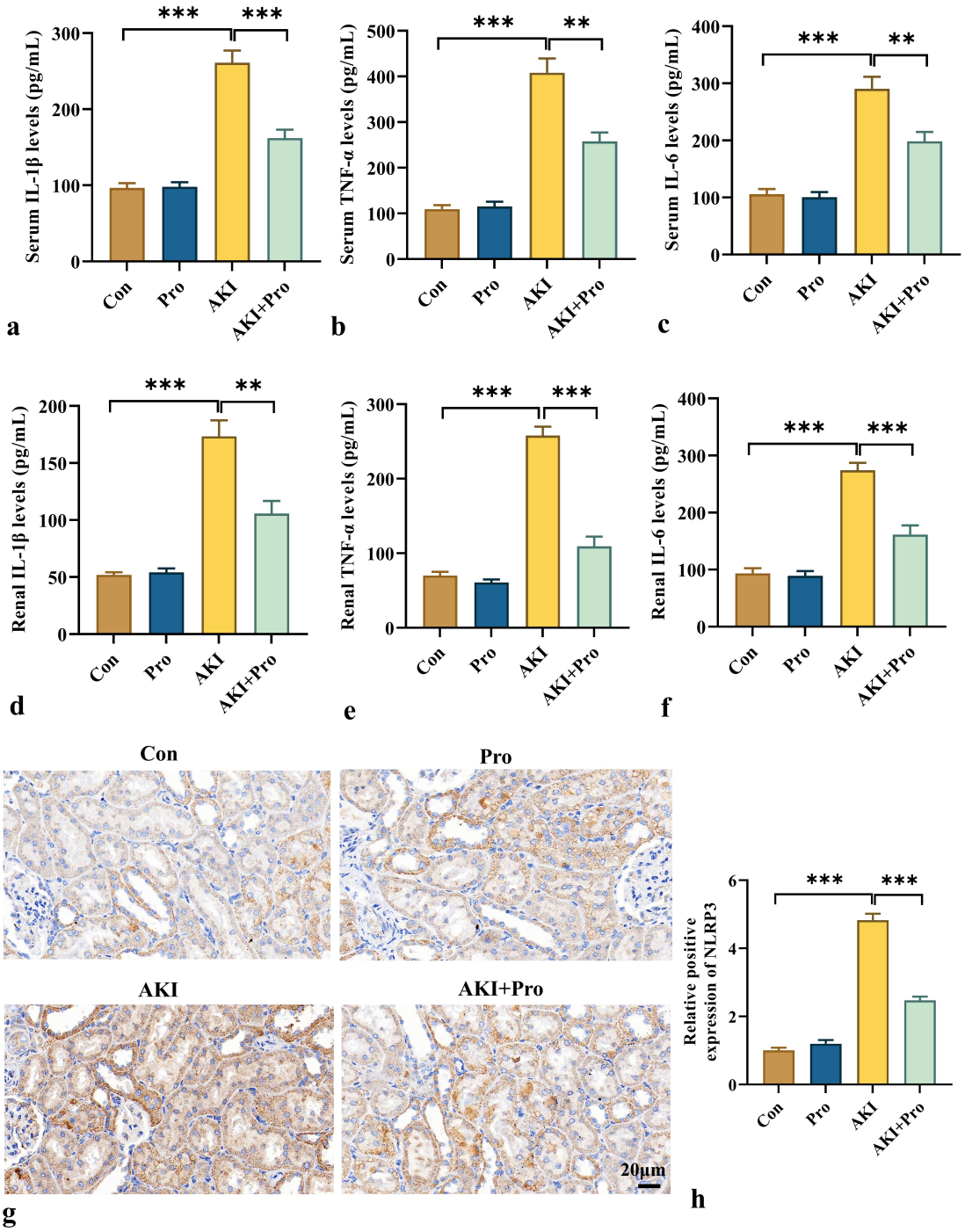


**Fig. 3. Propofol diminishes renal inflammatory response and inhibits NLRP3 inflammasome activation in AKI model mice.** (a–c) The IL-1$\beta$, TNF-$\alpha$, and IL-6 in the serum of mice in each group. (d–f) The IL-1$\beta$, TNF-$\alpha$, and IL-6 in the renal tissue of mice in each group. (g,h) Immunohistochemical detection of NLRP3 in each group (scale bar: 20 μm, magnification ×400). n = 6; $^{**}p < 0.01$, $^{***}p < 0.001$.

### *Propofol Protects Against LPS-induced HK-2 Cell Injury and Ferroptosis, With its Protective Effect Attenuated by Erastin*

The CCK-8 assay was used to detect the effect of different concentrations of propofol on the viability of LPS-treated HK-2 cells. The results showed that propofol treatment significantly enhanced cell viability. The most significant increase in cell viability was observed when the concentration of propofol was 10 μM ($p < 0.05$) [Fig. 4a]. Subsequently, 10μM of propofol was selected for treatment. However, from Fig. 4b, co-treatment with the ferroptosis inducer Erastin and LPS substantially weakened propofol's protective effect, as evidenced by a blunted recovery in cell viability ($p < 0.05$). Flow cytometry showed a marked increase in intracellular ROS production following LPS treatment, which was reduced by propofol pretreatment; this protective effect was compromised upon ferroptosis induction, as reflected by enhanced ROS generation ($p < 0.05$) [Fig. 4c,d]. WB analysis revealed significant downregulation of GPX4 and upregulation of the ferroptosis marker ACSL4 in LPS-stimulated HK-2 cells, which was reversed by propofol, confirming its protective role. However, compared with the propofol intervention group, the GPX4 expression was downregulated and the ACSL4 expression was upregulated in the LPS+Pro+Erastin group, indicating that ferroptosis was induced, and this weakened the suppression effect of propofol on ferroptosis ($p < 0.05$) [Fig. 4e,f].

### *Propofol Exerts its Protective Effect by Inhibiting LPS-induced Inflammatory Response in HK-2 Cells*

LPS stimulation led to a considerable increase of inflammatory factors such as TNF-$\alpha$, IL-1$\beta$, and IL-6 in the culture supernatant of HK-2 cells. However, propofol pretreatment could significantly reduce the levels of these inflammatory factors. Moreover, the addition of ferroptosis inducers resulted in a rebound in the secretion of inflammatory factors, indicating that the ferroptosis inducers enhanced the inflammatory response of the cells ($p < 0.05$) [Fig. 5a–c]. Consistent with the *in vivo* experiments, immunofluorescence detection showed that LPS stimulation also significantly enhanced the expression of NLRP3, while the NLRP3 expression in the LPS+Pro group cells was significantly decreased. Inducing ferroptosis caused the NLRP3 expression to rebound, further confirming that the protective effect of propofol is closely involved in the inhibition of the ferroptosis process ($p < 0.05$) [Fig. 5d,e].

## Discussion

This research comprehensively explored the protective role of propofol in AKI and its underlying mechanisms. The findings demonstrate that propofol notably enhances kidney function in mice with AKI and alleviates kidney tissue damage. The mechanism mainly involves inhibiting ferroptosis and inflammatory responses in renal tubular epithelial cells.

After the occurrence of AKI, the renal function is affected, manifested by elevated levels of urinary protein, Scr and BUN, and the swelling and necrosis of renal tubular epithelial cells. Propofol significantly improves renal tissue function following AKI, which is consistent with its protective effect demonstrated in previous studies [25]. In addition, for normal mouse models, propofol treatment had no effect on the various indicators of mouse renal function.

Mechanistically, the effect of propofol in improving renal function may be potentially explained by its ability to inhibit oxidative stress and ferroptosis. In this study, propofol significantly reduced the oxidative stress level in renal tissues, upregulated the GPX4 protein, downregulated the ACSL4 protein, and simultaneously reduced intracellular iron deposition, thereby inhibiting the occurrence of ferroptosis. This aligns with the results of Zhou *et al.* [19] in the sepsis-induced brain injury model, where propofol alleviated nerve injury and neuroinflammation by eliminating free radicals, inhibiting lipid peroxidation, and combating ferroptosis. Furthermore, *in vitro* experiments demonstrated that propofol could reduce the generation of ROS in HK-2 cells induced by LPS, further supporting its antioxidant properties. When Erastin was used to strongly induce ferroptosis, the protective effect of propofol weakened, which further verified that the inhibitory effect of propofol on ferroptosis was one of the important mechanisms for its protection against AKI.

This study further confirmed that propofol can reduce the levels of TNF-$\alpha$, IL-1$\beta$ and IL-6 in the serum and kidneys of AKI mice, and inhibit the activation of the NLRP3 inflammasome. This conforms with the findings of Liu *et al.* [34] in the lung injury model induced by renal ischemia and reperfusion, where propofol reduced the inflammatory cascade by inhibiting the NLRP3 inflammasome activation. It is worth noting that the NLRP3 inflammasome can simultaneously promote the release of inflammatory factors and the process of ferroptosis. The dual inhibition of propofol on both of these processes may form a synergistic protective effect [35]. For instance, Lu *et al.* [36] found that propofol reduced oxidative stress, inhibited ferroptosis and apoptosis, and simultaneously lowered inflammatory cytokines secretion to alleviate the cardiomyocyte toxicity induced by azithromycin.

Moreover, *in vitro* experiments showed that propofol pretreatment notably reduced the levels of inflammatory factors in the culture supernatant of HK-2 cells and weakened the immunofluorescence signal of NLRP3. The conclusions were similar in liver injury and cardiomyocyte injury models. For example, in the liver injury model, propofol inhibited the maturation of inflammatory and oxidative stress-related factors by blocking the NLRP3 pathway [37]. In the LPS-induced model of neonatal rat cardiomyocyte injury, propofol pretreatment reduced cardiomyocyte

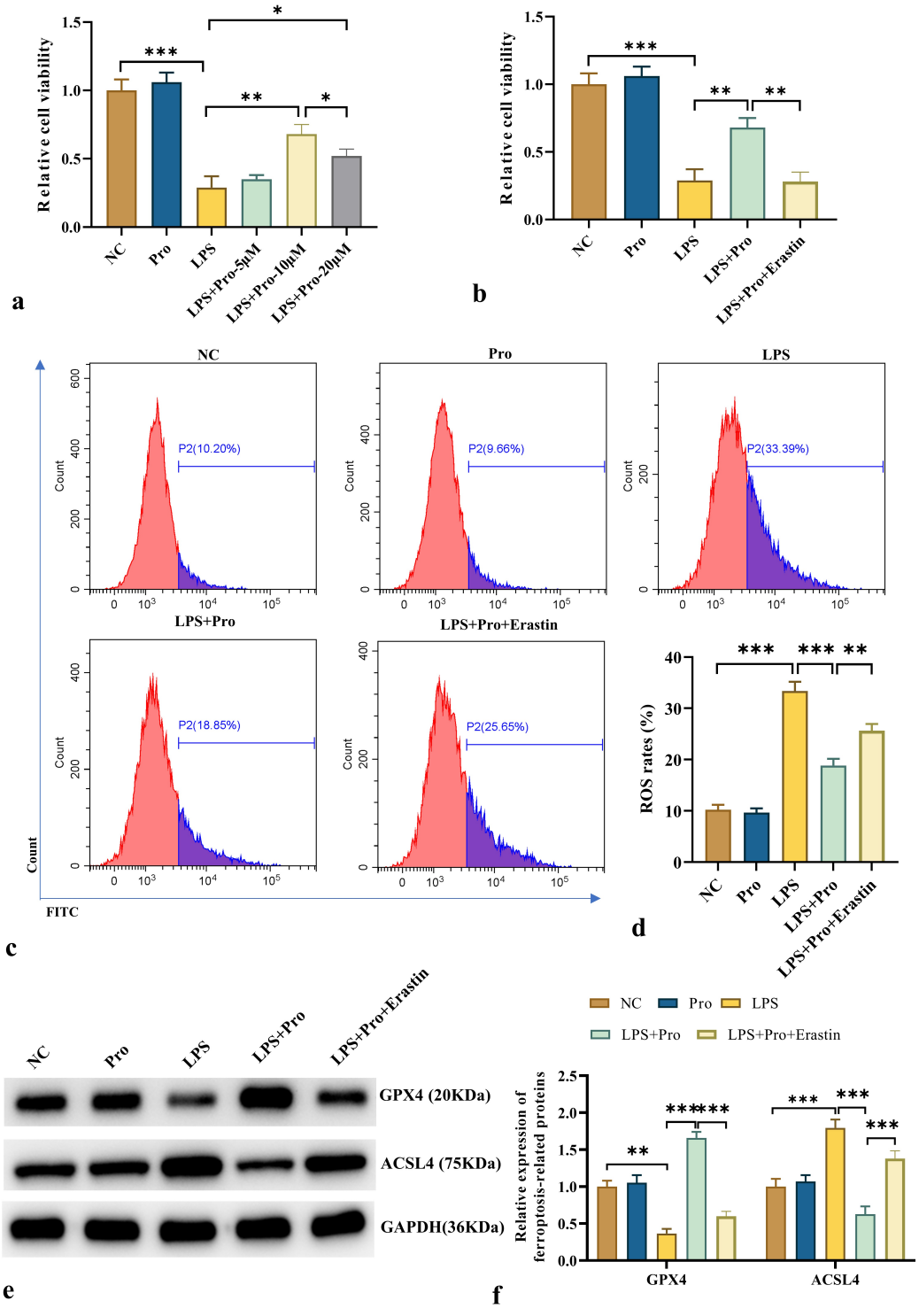


**Fig. 4. Propofol protects against LPS-induced HK-2 cell injury and ferroptosis, with its protective effect attenuated by Erastin.** (a,b) CCK-8 assay was used to detect the viability of cells in each group. (c,d) Flow cytometry was used to detect ROS levels in cells of each group. (e,f) The expression levels of the ferroptosis-related proteins ACLS4 and GPX4 were detected using WB analysis. n = 6; *$p < 0.05$, **$p < 0.01$, ***$p < 0.001$.

cell damage. The mechanism lies in which propofol inactivates the NLRP3 inflammatory body signaling pathway [38]. These findings suggest that propofol may be a therapeutic candidate for septic liver injury and myocardial damage. Additionally, this study also observed the correlation between inflammation inhibition and ferroptosis regulation. When Eastin was used to induce ferroptosis, the anti-inflammatory effect of propofol was simultaneously weak-

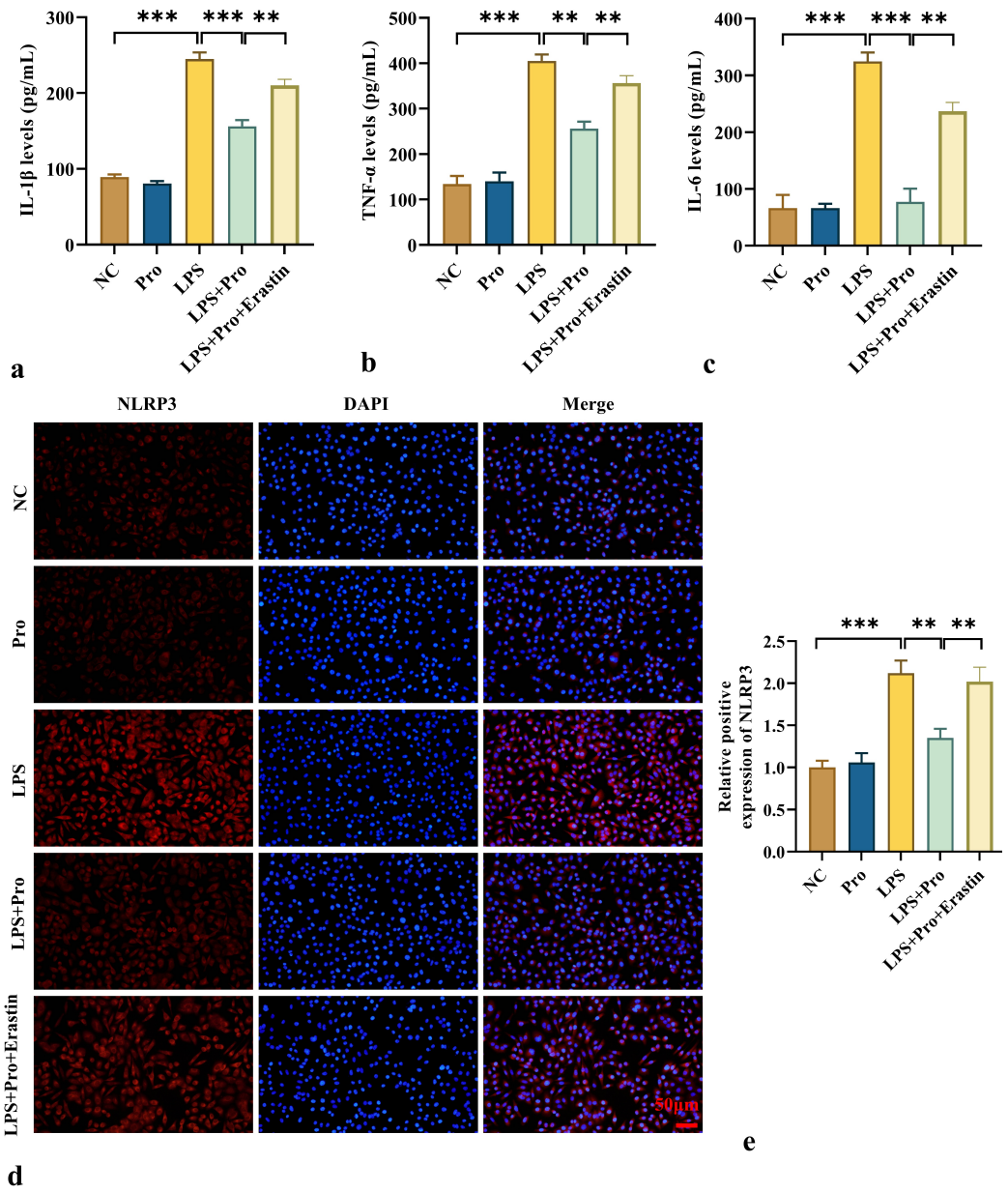


**Fig. 5. Propofol exerts its protective effect by inhibiting LPS-induced inflammatory response in HK-2 cells.** (a–c) ELISA was used to measure the levels of cytokines IL-1$\beta$, TNF-$\alpha$, and IL-6 in HK-2 cells. (d,e) Immunofluorescence was used to detect the expression of NLRP3 in HK-2 cells (scale bar: 50 µm, magnification ×200). n = 6; $^{**}p < 0.01$, $^{***}p < 0.001$.

ened, suggesting that ferroptosis may act as an upstream event to drive the inflammatory response. This dovetails with the theory proposed by Deng *et al*. [39] that "ferroptosis is a target for treating inflammatory diseases". Growing evidence indicates that ferroptosis inhibitors have potential benefits in treating inflammation, suggesting that targeting ferroptosis could be a promising approach for inflammatory diseases. Subsequent studies will need to further elucidate the specific molecular pathways regulating inflammation through the detection of indicators such as nuclear factor kappa-B (NF-$\kappa$B) p65 phosphorylation and I$\kappa$B$\alpha$ degradation.

This study also has certain limitations. Firstly, in the *in vivo* experiments, only the lipopolysaccharide-induced AKI model was used, which mainly simulates AKI related to infection and fails to cover other common causes, such as ischemia-reperfusion injury, renal toxicant-induced injury. Among the indicators for detecting ferroptosis, merely using Perls staining and WB to detect the relevant indicators may result in an incomplete assessment of ferroptosis. Therefore, the generalizability of the results needs to be further verified. Future studies could adopt multiple AKI models, such as ischemia-reperfusion-induced AKI, cisplatin-induced AKI, and ferroptosis detection methods for com-

parative research [40]. Secondly, although this study has revealed the inhibitory effect of propofol on ferroptosis and inflammatory responses, the specific molecular signaling pathways have not been fully elucidated. For instance, how propofol precisely regulates the expression of GPX4 and ACSL4 and its upstream regulatory mechanism on the NLRP3 signaling pathway still require in-depth investigation. In the future, through gene knockdown, overexpression experiments, and signal pathway inhibitors, etc., the detailed molecular mechanism of propofol exerting its protective effect can be further explored. It should be noted that Erastin may have a slight impact on cell death pathways other than ferroptosis. Subsequent studies could use the ferroptosis-specific inhibitor liproxstatin-1 to further verify the core role of ferroptosis in the protective effect of propofol, in order to rule out non-specific interference. Moreover, this study was conducted only in cellular and animal models, and clinical studies have not yet been carried out. The effectiveness and safety of propofol in the treatment of AKI in humans still need to be verified through clinical trials.

## Conclusions

In conclusion, this study has confirmed that propofol has a significant protective effect on AKI. This effect is mainly mediated by inhibition of ferroptosis and inflammatory responses in renal tubular epithelial cells. This study offers new insights and avenues for future research on the treatment strategies of AKI.

## Availability of Data and Materials

The data that support the findings of this study are available from the first author upon reasonable request.

## Author Contributions

JL and HHZ designed the research study. JL performed the research. JL and HHZ provided help and advice on the experiments. JL analyzed the data. Both authors contributed to the draft and critical revisions in the manuscript. Both authors read and approved the final manuscript. Both authors have participated sufficiently in the work and agreed to be accountable for all aspects of the work.

## Ethics Approval and Consent to Participate

The study has been approved by the Beijing Keweite Laboratory Animal Welfare Ethics Committee (Approval No. KWT-2024-0112-01).

## Acknowledgment

Not applicable.

## Funding

This research received no external funding.

## Conflict of Interest

The authors declare no conflict of interest.

## References

[1] Luo Y, Ye W, Sun Y, Bao H, Liu H. Development and Comparative Analysis of an Early Prediction Model for Acute Kidney Injury within 72-Hours Post-ICU Admission Using Evidence from the MIMIC-III Database. Discovery Medicine. 2023; 35: 623–631. https://doi.org/10.24976/Discov.Med.202335177.61.

[2] Ronco C, Bellomo R, Kellum JA. Acute kidney injury. Lancet (London, England). 2019; 394: 1949–1964. https://doi.org/10.1016/S0140-6736(19)32563-2.

[3] Pickkers P, Darmon M, Hoste E, Joannidis M, Legrand M, Ostermann M, *et al*. Acute kidney injury in the critically ill: an updated review on pathophysiology and management. Intensive Care Medicine. 2021; 47: 835–850. https://doi.org/10.1007/s00134-021-06454-7.

[4] Stanski NL, Rodrigues CE, Strader M, Murray PT, Endre ZH, Bagshaw SM. Precision management of acute kidney injury in the intensive care unit: current state of the art. Intensive Care Medicine. 2023; 49: 1049–1061. https://doi.org/10.1007/s00134-023-07171-z.

[5] Yao C, Li Z, Sun K, Zhang Y, Shou S, Jin H. Mitochondrial dysfunction in acute kidney injury. Renal Failure. 2024; 46: 2393262. https://doi.org/10.1080/0886022X.2024.2393262.

[6] Li ZL, Li XY, Zhou Y, Wang B, Lv LL, Liu BC. Renal tubular epithelial cells response to injury in acute kidney injury. EBioMedicine. 2024; 107: 105294. https://doi.org/10.1016/j.ebiom.2024.105294.

[7] Perazella MA. Drug-induced acute kidney injury: diverse mechanisms of tubular injury. Current Opinion in Critical Care. 2019; 25: 550–557. https://doi.org/10.1097/MCC.0000000000000653.

[8] Li X, Yuan F, Xiong Y, Tang Y, Li Z, Ai J, *et al*. FAM3A plays a key role in protecting against tubular cell pyroptosis and acute kidney injury. Redox Biology. 2024; 74: 103225. https://doi.org/10.1016/j.redox.2024.103225.

[9] Newton K, Strasser A, Kayagaki N, Dixit VM. Cell death. Cell. 2024; 187: 235–256. https://doi.org/10.1016/j.cell.2023.11.044.

[10] Shafiee L, Pishva MS, Hosseinzadegsn R, Bahadori Z, Baziyar P, Mehboodi M, *et al*. Hesperetin reduces neuronal death in an SHSY5Y Alzheimer's model by inhibiting inflammation and apoptosis and pyroptosis cell death pathways. Scientific Reports. 2025; 15: 41901. https://doi.org/10.1038/s41598-025-25777-9.

[11] Liu W, Chen B, Wang Y, Meng C, Huang H, Huang XR, *et al*. RGMb protects against acute kidney injury by inhibiting tubular cell necroptosis via an MLKL-dependent mechanism. Proceedings of the National Academy of Sciences of the United States of America. 2018; 115: E1475–E1484. https://doi.org/10.1073/pnas.1716959115.

[12] Martin-Sanchez D, Ruiz-Andres O, Poveda J, Carrasco S, Cannata-Ortiz P, Sanchez-Niño MD, *et al*. Ferroptosis, but Not Necroptosis, Is Important in Nephrotoxic Folic Acid-Induced AKI. Journal of the American Society of Nephrology: JASN. 2017; 28: 218–229. https://doi.org/10.1681/ASN.2015121376.

[13] Qiao O, Wang X, Wang Y, Li N, Gong Y. Ferroptosis in acute kidney injury following crush syndrome: A novel target for treatment. Journal of Advanced Research. 2023; 54: 211–222. https://doi.org/10.1016/j.jare.2023.01.016.

[14] Wang Y, Zhang M, Bi R, Su Y, Quan F, Lin Y, *et al*. ACSL4 deficiency confers protection against ferroptosis-mediated acute kidney injury. Redox Biology. 2022; 51: 102262. https://doi.org/10.1016/j.redox.2022.102262.

[15] Zheng Q, Xing J, Li X, Tang X, Zhang D. PRDM16 suppresses ferroptosis to protect against sepsis-associated acute kidney injury by targeting the NRF2/GPX4 axis. Redox Biology. 2024; 78: 103417. https://doi.org/10.1016/j.redox.2024.103417.

[16] Fu Y, Xiang Y, Li H, Chen A, Dong Z. Inflammation in kidney repair: Mechanism and therapeutic potential. Pharmacology & Therapeutics. 2022; 237: 108240. https://doi.org/10.1016/j.pharmthera.2022.108240.

[17] Yang YY, Ye L, Chen J, Qiu Y, Yin YL, Li P. Dok3 is involved in cisplatin-induced acute kidney injury via regulation of inflammation and apoptosis. Biochemical and Biophysical Research Communications. 2021; 569: 132–138. https://doi.org/10.1016/j.bbrc.2021.06.097.

[18] Heiberg J, Royse CF, Royse AG, Andrews DT. Propofol Attenuates the Myocardial Protection Properties of Desflurane by Modulating Mitochondrial Permeability Transition. Anesthesia and Analgesia. 2018; 127: 387–397. https://doi.org/10.1213/ANE.0000000000003450.

[19] Zhou Y, Yang Y, Yi L, Pan M, Tang W, Duan H. Propofol Mitigates Sepsis-Induced Brain Injury by Inhibiting Ferroptosis Via Activation of the Nrf2/HO-1axis. Neurochemical Research. 2024; 49: 2131–2147. https://doi.org/10.1007/s11064-024-04163-3.

[20] Liu X, Yang B, Tan YF, Feng JG, Jia J, Yang CJ, *et al*. The role of AMPK-Sirt1-autophagy pathway in the intestinal protection process by propofol against regional ischemia/reperfusion injury in rats. International Immunopharmacology. 2022; 111: 109114. https://doi.org/10.1016/j.intimp.2022.109114.

[21] Zhang J, Chen A, Song Y. Propofol Triggers Cell Death in Lung Cancer Cells by Increasing PANX1 Expression, Activating the Mitochondrial Cell Death Pathway, and Enhancing ROS Levels. Discovery Medicine. 2024; 36: 2231–2243. https://doi.org/10.24976/Discov.Med.202436190.205

[22] Hausburg MA, Banton KL, Roman PE, Salgado F, Baek P, Waxman MJ, *et al*. Effects of propofol on ischemia-reperfusion and traumatic brain injury. Journal of Critical Care. 2020; 56: 281–287. https://doi.org/10.1016/j.jcrc.2019.12.021.

[23] Wu J, Yu C, Zeng X, Xu Y, Sun C. Protection of propofol on liver ischemia reperfusion injury by regulating Cyp2b10/ Cyp3a25 pathway. Tissue & Cell. 2022; 78: 101891. https://doi.org/10.1016/j.tice.2022.101891.

[24] Liu Z, Li C, Li Y, Yu L, Qu M. Propofol Reduces Renal Ischemia Reperfusion-mediated Necroptosis by Up-regulation of SIRT1 in Rats. Inflammation. 2022; 45: 2038–2051. https://doi.org/10.1007/s10753-022-01673-6.

[25] Zheng G, Qu H, Li F, Ma W, Yang H. Propofol attenuates sepsis-induced acute kidney injury by regulating miR-290-5p/CCL-2 signaling pathway. Brazilian Journal of Medical and Biological Research = Revista Brasileira De Pesquisas Medicas E Biologica. 2018; 51: e7655. https://doi.org/10.1590/1414-431X20187655.

[26] Wei Q, Zhao J, Zhou X, Yu L, Liu Z, Chang Y. Propofol can suppress renal ischemia-reperfusion injury through the activation of PI3K/AKT/mTOR signal pathway. Gene. 2019; 708: 14–20. https://doi.org/10.1016/j.gene.2019.05.023.

[27] Zhang B, Zeng M, Wang Y, Li M, Wu Y, Xu R, *et al*. Oleic acid alleviates LPS-induced acute kidney injury by restraining inflammation and oxidative stress via the Ras/MAPKs/PPAR-$\gamma$ signaling pathway. Phytomedicine: International Journal of Phytotherapy and Phytopharmacology. 2022; 94: 153818. https://doi.org/10.1016/j.phymed.2021.153818.

[28] Sun J, Ge X, Wang Y, Niu L, Tang L, Pan S. USF2 knockdown downregulates THBS1 to inhibit the TGF-$\beta$ signaling pathway and reduce pyroptosis in sepsis-induced acute kidney injury. Pharmacological Research. 2022; 176: 105962. https://doi.org/10.1016/j.phrs.2021.105962.

[29] Wang D, Jin M, Zhao X, Zhao T, Lin W, He Z, *et al*. FGF1$^{HBS}$ ameliorates chronic kidney disease via PI3K/AKT mediated suppression of oxidative stress and inflammation. Cell Death & Disease. 2019; 10: 464. https://doi.org/10.1038/s41419-019-1696-9.

[30] Yao M, Wu Y, Cao Y, Liu H, Ma N, Chai Y, *et al*. Autophagy-Mediated Clearance of Free Genomic DNA in the Cytoplasm Protects the Growth and Survival of Cancer Cells. Frontiers in Oncology. 2021; 11: 667920. https://doi.org/10.3389/fonc.2021.667920.

[31] Li W, Hao X, Liu Y, Tong T, Xu H, Jia L. Effects of anesthetic agents on inflammation in Caco-2, HK-2 and HepG2 cells. Experimental and Therapeutic Medicine. 2021; 21: 487. https://doi.org/10.3892/etm.2021.9918.

[32] Luo X, Zhao Y, Luo Y, Lai J, Ji J, Huang J, *et al*. Cytosolic mtDNA-cGAS-STING axis contributes to sepsis-induced acute kidney injury via activating the NLRP3 inflammasome. Clinical and Experimental Nephrology. 2024; 28: 375–390. https://doi.org/10.1007/s10157-023-02448-5.

[33] Sun F, He Y, Yang Z, Xu G, Wang R, Juan Z, *et al*. Propofol pretreatment inhibits ferroptosis and alleviates myocardial ischemia-reperfusion injury through the SLC16A13-AMPK-GPX4 pathway. Biomedicine & Pharmacotherapy = Biomedecine & Pharmacotherapie. 2024; 179: 117345. https://doi.org/10.1016/j.biopha.2024.117345.

[34] Liu Z, Meng Y, Miao Y, Yu L, Yu Q. Propofol reduces renal ischemia/reperfusion-induced acute lung injury by stimulating sirtuin 1 and inhibiting pyroptosis. Aging. 2020; 13: 865–876. https://doi.org/10.18632/aging.202191.

[35] Zhang Z, He Y, Liu H, Liu Y, Wu T, Li R, *et al*. NLRP3 regulates ferroptosis via the JAK2/STAT3 pathway in asthma inflammation: Insights from in vivo and in vitro studies. International Immunopharmacology. 2024; 143: 113416. https://doi.org/10.1016/j.intimp.2024.113416.

[36] Lu Z, Liu Z, Fang B. Propofol protects cardiomyocytes from doxorubicin-induced toxic injury by activating the nuclear factor erythroid 2-related factor 2/glutathione peroxidase 4 signaling pathways. Bioengineered. 2022; 13: 9145–9155. https://doi.org/10.1080/21655979.2022.2036895.

[37] Zhang Z, Tian L, Jiang K. Propofol attenuates inflammatory response and apoptosis to protect d-galactosamine/lipopolysaccharide induced acute liver injury via regulating TLR4/NF-κB/NLRP3 pathway. International Immunopharmacology. 2019; 77: 105974. https://doi.org/10.1016/j.intimp.2019.105974.

[38] Zhao H, Gu Y, Chen H. Propofol ameliorates endotoxin induced myocardial cell injury by inhibiting inflammation and apoptosis via the PPARγ/HMGB1/NLRP3 axis. Molecular Medicine Reports. 2021; 23: 176. https://doi.org/10.3892/mmr.2020.11815.

[39] Deng L, He S, Guo N, Tian W, Zhang W, Luo L. Molecular mechanisms of ferroptosis and relevance to inflammation. Inflammation Research. 2023; 72: 281–299. https://doi.org/10.1007/s00011-022-01672-1.

[40] Zhang T, Widdop RE, Ricardo SD. Transition from acute kidney injury to chronic kidney disease: mechanisms, models, and biomarkers. American Journal of Physiology. Renal Physiology. 2024; 327: F788–F805. https://doi.org/10.1152/ajprenal.00184.2024.